Feasibility Study of Tumor Monitoring Technique using Prompt Gamma Rays during Antiproton Therapy

*Han-Back Shin, Do-Kun Yoon, Tae Suk Suh**
Department of Biomedical Engineering and Research Institute of Biomedical Engineering, College of Medicine, Catholic University of Korea, Seoul 505, Kroea
**Corresponding author: suhsanta@catholic.ac.kr*

1. Introduction

The antiproton, the stable antiparticle of the proton, has the same physical characteristics of the proton, but carries a negative charge and different magnetic moment [1]. Antiprotons are generated by accelerating protons which accelerated to 26 GeV/c in a proton synchrotron to strike a fixed target; the collision produces a small quantity of antiprotons (less than 1%) [1]. Consequently, some researchers concluded that they could be applied in radiation therapy [1,2]. The biologically effective dose ratio has showed that the antiproton is four times more effective than the conventional proton for cell irradiation [3-5]. Tumor monitoring using the prompt gamma ray presents several advantages. First, the region accuracy of the irradiation can be evaluated during the treatment. In case of inaccuracy, the therapy can be stopped immediately. Second, as the status of the tumor under treatment can be confirmed, the accuracy of the treatment level can be analyzed, and the prognosis estimated. Third, the radiation treatment planning for the next therapy can be easily corrected through the reflection based on the prognosis from the previous prompt gamma ray imaging.

Briefly, the purpose of this study is to verify the effectiveness of the antiproton boron fusion therapy and the acquisition of the tumor image by using the prompt gamma ray emission during the treatment.

2. Methods and Results

We used the Monte Carlo N-particle extended (MCNPX, Ver. 2.6.0, Los Alamos National Laboratory, Los Alamos, NM, USA) simulation code to prove the correctness of the concept at the basis of the proposed monitoring technique [6].

The cylindrical water phantom (density= 1 g/cm^3) had a diameter of 160.0 mm and a height of 100.0 mm [8]. The three different-sized BURs were placed at different locations, and denoted as region A (diameter = 20.0 mm, x = 15.0 mm, y = − 13.2 mm), region B (diameter = 15.0 mm, x = − 18.9 mm, y = − 6.4 mm), and region C (diameter = 10.0 mm, x = 3.9 mm, y = 19.6 mm). The height of the three BURs was 20.0 mm. The boron concentration was 780 μg/g; this value was derived from a previous BNCT study on the clinical use of boron concentration.

For the operation of the MCNPX, the concept of boron concentration should be defined as the density. When the boron particles were stacked at the tumor, the tumor volume had an average density of 2.0 g/cm^3. This value is sufficiently differs in relation to the conditions (e.g., patient, metabolism, etc.), and it is not an absolute standard.

As the 719 keV prompt gamma ray is a single photon, a four head SPECT system was used to acquire the tomographic image of the identified tumor region. Typically, conventional SPECT is used to detect low energy photons (< 500 keV). As 719 keV is relatively high photon energy, the design of a collimator and high-density detector material had to be considered. In our simulation, to simulate the SPECT system, we used a tungsten (density = 17.3 g/cm^3) parallel collimator with a thickness of 2.5 mm and lutetium yttrium oxyorthosilicate (LYSO, density = 7.3 g/cm^3) detector material with a thickness of 30 mm. The flux of the antiproton source was set at 2.56 × 10^{10} n/cm^2·s, which sufficiently covered the BURs. Fig. 1 shows a diagram of the simulation setup, including the SPECT system, the phantom, and the antiproton therapy system. The schematic in the inset illustrates the atomic reaction occurring between antiproton and boron.

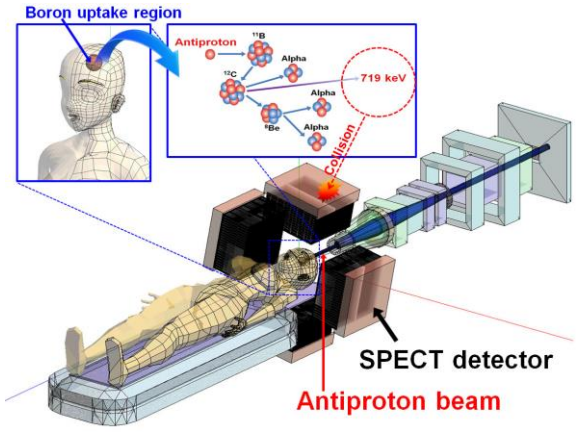

Fig. 1. Diagram of Monte Carlo simulation for the reaction between antiproton and boron. The water phantom, including three boron uptake regions (BURs; red regions), is located at the center of the four head single photon emission computed tomography system. The antiproton beam reacts with the boron particles at the BURs. The emission of the 719 keV prompt gamma ray is illustrated in the inset.

The energy spectrum of the prompt gamma ray emitted during the reaction between antiproton and boron was deduced using the F8 tally function (energy deposition tally) of the MCNPX code [6]. Furthermore, the percentage depth dose (PDD) of the antiproton was extracted from the water phantom, including the BURs, using the F6 tally function (absorbed dose tally) of the MCNPX code [6]. The acquisition of the tomographic image to monitor the tumor during the treatment required a SPECT scan with a low projection number.

The events of the 719 keV prompt gamma ray for imaging were collected using a 10% energy window. To quantitatively assess the tomographic image quality, the signal-to-noise ratio (SNR) and contrast-to-noise ratio (CNR) were calculated within the BURs of the spherical phantom [7,8]. The SNR of the images was deducted by the circular region of interest (ROI) placed in the BURs. The SNR of the ROI was calculated by the standard deviation (SD) of the mean pixel value [7]. The CNR, which is the ratio of the signal change of an object of interest, was calculated by dividing the difference of the signal ratio between the BURs by the SD of the background noise [8].

The receiver operating characteristic (ROC) curve was used to analyze the accuracy of the reconstructed image.

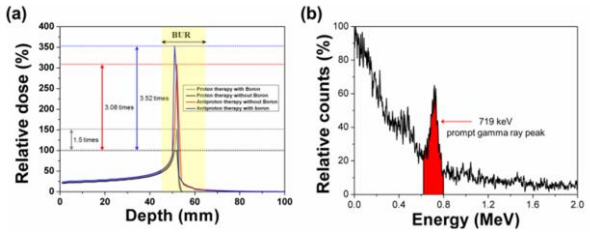

Fig. 2. Percentage depth dose (PDD) of proton and antiproton beams and energy spectrum of prompt gamma ray.
(a) Percentage depth dose (PDD) of proton and antiproton beams from the water phantom with and without boron uptake regions (BURs). The black line indicates the PDD of a conventional proton beam from the water phantom without BURs, whereas the gray, red and blue lines indicate the PDDs of the proton beam with BURs and the antiproton beam from the water phantom without and with BURs, respectively. (b) Energy spectrum of prompt gamma ray from the reaction between antiproton and boron; the 719 keV prompt gamma ray peak is clearly visible. The red region indicates the energy window for the reconstruction image.

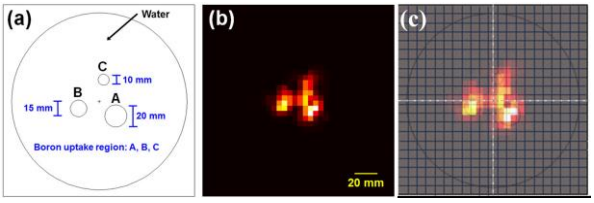

Fig. 3. Reconstruction image using prompt gamma ray originated from antiproton boron fusion reaction.
(a) Original pattern of the water phantom including the three boron uptake regions (BURs). (b) Reconstructed image using the 719 keV prompt gamma ray events induced by the reaction between antiprotons and boron (32 projections). (c) Three black circular lines are the ROI for ROC calculation. This circular line was compared with reconstructed image of BURs for ROC calculation using pixel matching method.

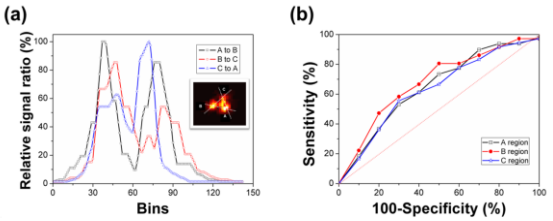

Fig. 4. Quantitative analysis of prompt gamma ray image.
(a) Image profiles of three lines in the reconstructed image: the black line indicates the image profile from region C to region B, the red line indicates the image profile from region C to region A, and the blue line indicates the image profile from region B to region A. (b) Receiver operating characteristic (ROC) curve regarding the three boron uptake regions. The values of the areas under the ROC curve (AUC) were 0.647 (region A, black line), 0.679 (region B, red line), and 0.632 (region C, blue line).

3. Conclusions

The treatment of a tumor using an antiproton beam with boron particles has clearly positive effects. First, the proton maximum dose level can be increased by the antiproton boron fusion reaction, and a more critical dose can be transferred to the tumor than that delivered in conventional antiproton therapy or proton therapy. Second, tumor monitoring using the prompt gamma rays produced by the reaction between the antiprotons and the boron is possible during the treatment, and can provide the guidance for a more accurate radiation therapy. In future work, further simulation studies including a clinical factors will be performed.

REFERENCES

[1] F. H. Ruddy, A. R. Dulloo, J. G. Seidel, F. W, Hantz, and L. R. Grobmyer, Nuclear Reactor Power Monitoring Using Silicon Carbide Semiconductor Radiation Detectors, Nuclear Technology, Vol.140, p. 198, 2002.
[1] Chamberlain O, Segrè E, Wiegand C, Ypsilantis T. Observation of Antiprotons. Phys Rev. 1955;100: 947-950.
[2] Gray L, Kalogeropoulos TE. Possible biomedical application of antiproton beams: focused radiation transfer. Radiat Res. 1984;97: 246-250.
[3] Holzscheiter MH, Agazarayan N, Bassler N, Beyer G, DeMarco JJ, Doser M, et al. Biological effectiveness of antiproton annihilation. Nucl Instrum Methods Phys Res B. 2004;221: 210-214.
[4] Maggiore C, Agazarayan N, Bassler N, Blackmore E, Beyer G, DeMarco JJ, et al. Biological effectiveness of antiproton annihilation. Nucl Instrum Methods Phys Res

B. 2004;214: 181-185.
[5] Holzscheiter MH, Bassler N, Agazaryan N, Beyer G, Blackmore E, DeMarco JJ, et al. The biological effectiveness of antiproton irradiation. Radiother Oncol. 2006;81: 233.
[6]Yoon DK, Jung JY, Suh TS. Application of proton boron fusion reaction to radiation therapy: A Monte Carlo simulation study. Appl Phys Lett. 2014;105: 223507.
[7] Hong KJ, Choi Y, Jung JH, Kang J, Hu W, Lim HK, et al. A prototype MR insertable brain PET using tileable GAPD arrays. Med Phys. 2013;40: 042503.
[8] Antoch G, Freudenberg LS, Stattaus J, Jentzen W, Mueller SP, Debatin JF, et al. Whole-Body Positron Emission Tomography—CT: Optimized CT Using Oral and IV Contrast Materials. Am J Roentgenol. 2002;179: 1550-1560.